Materials Science and Engineering C 35 (2014) 253–258

Contents lists available at ScienceDirect

Materials Science and Engineering C

journal homepage: www.elsevier.com/locate/msec

A novel acetylcholinesterase biosensor based on carboxylic graphene coated with silver nanoparticles for pesticide detection

Yongjun Liu [a], Guangcan Wang [a,*], Canpeng Li [a], Qing Zhou [b], Min Wang [a], Long Yang [a]

[a] School of Chemical Science and Engineering, Yunnan University, Kunming 650091, China
[b] School of Physical Science and Technology, Yunnan University, Kunming 650091, China

ARTICLE INFO

Article history:
Received 4 May 2013
Received in revised form 12 September 2013
Accepted 31 October 2013
Available online 14 November 2013

Keywords:
Silver nanoparticles
Carboxylic graphene
Nafion
Acetylcholinesterase biosensor

ABSTRACT

A novel acetylcholinesterase (AChE) biosensor based on Ag NPs, carboxylic graphene (CGR) and Nafion (NF) hybrid modified glass carbon electrode (GCE) has been successfully developed. Ag NPs–CGR–NF possessed predominant conductivity, catalysis and biocompatibility and provided a hydrophilic surface for AChE adhesion. Chitosan (CS) was used to immobilize AChE on the surface of Ag NPs–CGR–NF/GCE to keep the AChE activities. The AChE biosensor showed favorable affinity to acetylthiocholine chloride (ATCl) and could catalyze the hydrolysis of ATCl with an apparent Michaelis–Menten constant value of 133 μM, which was then oxidized to produce a detectable and fast response. Under optimum conditions, the biosensor detected chlorpyrifos and carbaryl at concentrations ranging from 1.0×10^{-13} to 1×10^{-8} M and from 1.0×10^{-12} to 1×10^{-8} M. The detection limits for chlorpyrifos and carbaryl were 5.3×10^{-14} M and 5.45×10^{-13} M, respectively. The developed biosensor exhibited good sensitivity, stability, reproducibility and low cost, thus providing a promising tool for analysis of enzyme inhibitors. This study could provide a simple and effective immobilization platform for meeting the demand of the effective immobilization enzyme on the electrode surface.

1. Introduction

Organophosphate and carbamate pesticides are widely used as insecticides in order advance crop yield. Unfortunately, these pesticides exhibit high acute toxicity, with the majority being hazardous to human and animal health. Indeed, the inhibition of acetylcholinesterase (AChE) activity by pesticides can lead to a disturbance of normal neuronal function and possibly death [1,2]. The exact and speedy measurement of pesticides in water and food is of great importance. Biosensors based on AChE have emerged as a promising technique for toxicity analysis, environmental monitoring, foodstuff quality and military investigations in recent years [3,4]. The main application of AChE biosensors is for the detection of pesticides based on enzyme inhibition. The biosensors are designed to complement or replace the existing reference analytical methods such as HPLC, GC, and GC/MS by simplifying sample preparation and analytic process, thus decreasing the analysis time and cost. Our research purpose is to develop a sensitive and stable AChE biosensor for detection of pesticides to reach the same level of these analytical instruments.

Graphene (GR), a two-dimensional sheet of sp2-bonded carbon atoms arranged in a honeycomb lattice, has attracted increasing attention since it was first isolated from three-dimensional graphite by mechanical exfoliation [5]. Due to its extraordinary thermal, mechanical, electrical and electrochemical properties, GR is usually considered as a competitive candidate for next-generation electronic and electrochemical applications such as super-capacitors [6,7], batteries [8,9], fuel cells [10,11], solar cells [12,13], catalysts [14,15], sensors [16,17], and biosensors [18,19]. However, many researches have reported that the pure GR actually exhibits unsatisfactory electrical conductivity and electrochemical catalytic activity because of the inevitable aggregation. Some of the useful and unique properties of GR such as conductivity and catalysis can only be realized after it is functionalized with organic groups such as hydroxyl, carboxyl, amino and the like. Functionalized GR sheets are easier to disperse in organic solvents, which can improve the dispersion and conductivity [20,21].

It is well known that Ag NPs possess high conductivity, surface area, excellent catalytic activity, and biocompatibility. Ag NPs exhibit high catalytic activity for hydrogen peroxide reduction [22,23], and Ag NPs could provide a suitable microenvironment to retain biological activity for biomolecule immobilization [24]. Ag NPs facilitate more efficient electron transfer between the immobilized biomolecules and electrode substrates. This has led to the construction of electrochemical biosensors with enhanced analytical performance using Ag NPs [25,26].

Chitosan (CS) is an abundant natural biopolymer with excellent film forming ability, biocompatibility and nontoxicity, provides natural microenvironment to the enzyme and also gives sufficient accessibility to electrons to shuttle between the enzyme and the electrode [27]. For example, an amperometric glucose biosensor based on immobilization of glucose oxidase in CS on a glassy carbon electrode modified with gold–platinum alloy NPs/multiwall carbon nanotubes with a high sensitivity, good reproducibility, stability and selectivity [28]. Recently, an

* Corresponding author at: 2 North Cuihu Road, Kunming 650091, China. Tel.: +86 871 5033218; fax: +86 871 5153832.
E-mail address: wangc166163@sina.com (G. Wang).

0928-4931/$ – see front matter © 2013 Elsevier B.V. All rights reserved.
http://dx.doi.org/10.1016/j.msec.2013.10.036

amperometric biosensor was developed for ethanol detection by co-immobilizing multiwalled carbon nanotubes (MWCNTs) and alcohol dehydrogenase (ADH) within a CS matrix on a glassy carbon electrode [29]. And also, an optical biosensor based on glutamate dehydrogenase immobilized in a CS film was developed for the determination of ammonium in water samples [30].

Based on the above research results, Ag NPs and CGR have been synthesized which Ag NPs can be equably separated and anchored on carboxylic graphene (CGR) and dispersed in Nafion (NF). In this work, a novel AChE biosensor has been developed based on Ag NPs–CGR–NF modified GCE. The Ag NPs–CGR nanocomposites were homogeneously dispersed in NF then modified on the surface of GCE and formed symmetrical membrane which possessed excellent conductivity, catalytic activity, and biocompatibility which were attributed to the synergistic effects of Ag NPs, CGR and NF and provided a hydrophilic surface for AChE adhesion. Furthermore, CS was used to immobilize AChE on the surface of Ag NPs–CGR–NF/GCE to keep the AChE activities and assist electrons to shuttle between the enzyme and CGR–NF/GCE. Finally, NF was used as a protective membrane of the AChE biosensors to improve the stability of the biosensor. The biosensor exhibited excellent affinity to its substrate and the catalytic effect on the hydrolysis of ATCl. The biosensor has been demonstrated as a device with high sensitivity, acceptable stability and reproducibility for the analysis of ATCl and pesticides. More importantly, this study provides a universal and effective platform for meeting the demand of the effective immobilization enzyme on the Ag NPs–CGR–NF/GCE surface.

2. Experimental

2.1. Chemicals

Acetylcholinesterase (AChE Type C3389, 500 U/mg from electric eel), Acetylthiocholine chloride (ATCl), Chitosan (CS 85% deacetylation) and Nafion (NF 5% in lower aliphatic alcohols and water) were purchased from Sigma-Aldrich (St. Louis, USA). Chlorpyrifos and carbaryl (99.99%) were obtained from AccuStandard (USA). Graphite powder was purchased from Sinopharm Chemical Reagent Company (China). $AgNO_3$ was obtained from Shanghai Chemical Reagent Co. Ltd. (China). All other reagents were of analytical grade and obtained from Shanghai Chemical Reagent Co. Ltd. (China). Aqueous solutions were prepared with deionized (DI) water (18 MΩ cm).

2.2. Preparation of CGR

Graphite oxide prepared by Hummers' method [31] was suspended in water and exfoliated through ultrasonication for 2 h to obtain graphene oxide (GO) solution. GO solution was centrifuged at 3000 rpm to remove unexfoliated graphite oxide. CGR was prepared as reported [32] with the modification of replacing the method of drying in an oven with vacuum freeze-drying. Briefly, GO aqueous suspension (5 ml) was diluted to give a concentration of 2.0 mg/ml, and then sonicated for 1 h to give a clear solution. 1.2 g of NaOH and 1.0 g chloroacetic acid (Cl–CH_2–COOH) were added to the suspension and sonicated for 3 h to convert the −OH groups to −COOH via conjugation of acetic acid moieties. Sequentially the suspension was separated by centrifuging at a speed of 15,000 rpm, washed with DI water for several cycles. After vacuum freeze-drying, CGR was obtained.

2.3. Synthesis of Ag NPs–CGR nanocomposites

The Ag NPs–CGR nanocomposites were prepared as follows: briefly, 2.0 mg CGR was suspended in 2.0 ml of 0.46 mM $AgNO_3$ by sonicating for 10 min to disperse CGR equably. Then 1.0 ml of 0.01 M sodium citrate and 4.0 ml ethanol were added to the above suspension. Ice-cold, freshly prepared 1.0 ml of 0.01 M $NaBH_4$ solution was added to the above mixture while stirring until the color of the solution did not change. After stirring for an additional 10 h, the suspension was separated by centrifuging at a speed of 12,000 rpm, washed with DI water for several cycles. After vacuum freeze-drying, Ag NPs–CGR nanocomposites were obtained.

2.4. Preparation of biosensors

NF solution (0.125%, Wt/V) was prepared by diluting 5% of NF with ethanol and DI water (V/V, 1/1). The Ag NPs–CGR (0.5 mg) were added to 1.0 ml of the NF solution and sonicated thoroughly until a homogeneous suspension of Ag NPs–CGR–NF obtained. Similarly 0.5 mg/ml CGR–NF and GO–NF homogeneous suspension was obtained, respectively. The suspensions were stored under refrigeration at 4 °C. A GCE was polished carefully to a mirror-like with 0.3 and 0.05 μm alumina slurry and sequentially sonicated for 3 min in nitric acid (V/V, 1/1), ethanol and water. Before the experiment, the electrode was scanned from −0.1 to +1.1 V until a steady-state current–voltage curve was obtained. The Ag NPs–CGR–NF/GCE was prepared by dropping 5 μl of 0.5 mg/ml Ag NPs–CGR–NF suspension onto the surface of GCE and drying at room temperature. A similar method was used to prepare CGR–NF/GCE and GO–NF/GCE. The enzyme solution was mixed with 0.05 U AChE and 0.2% CS (Wt/V, 50 mM acetic acids). The modified electrodes were each coated 4.5 μl of AChE–CS (V/V, 2/1) and dried at 4 °C. The AChE–CS/GO–NF/GCE, AChE–CS/CGR–NF/GCE and AChE–CS/Ag NPs–CGR/GCE biosensors were obtained and washed with 0.1 M PBS to remove the unbound AChE. Finally, three types of biosensor were each covered with 3 μl 0.1% (Wt/V) NF as the protective membrane. Thus, three types of biosensor structure were NF/AChE–CS/GO–NF/GCE, NF/AChE–CS/CGR–NF/GCE and NF/AChE–CS/Ag NPs–CGR/GCE. Similarly, NF/AChE–CS/GCE was produced as a control.

2.5. Material characterization

Scanning electron microscopy (SEM, QUNT200 USA), scanning probe microscopy (SPM, SPA400) and transmission electron microscopy (TEM, Tecnai G F30 USA) were used to characterize CGR and Ag NPs–CGR morphologies. Raman spectra (Raman Station 400F PERKINELMER USA) and Fourier transform infrared spectra (FTIR, Thermo Fisher SCIENTIFIC Nicolet IS10 USA) were used to study the GO and CGR. An X-ray diffractometer (XRD, Rigaku TTR III Japan) was used to identify the phase of Ag NPs on CGR sheets. The solution CGR and Ag NPs–CGR 0.5 mg/ml of DI water respectively were used for SEM, AFM and TEM detection. GO and CGR which were not treated were used for Raman spectra detection. GO and CGR which were mixed with a fix quantity of potassium bromide were used for Fourier transform infrared spectrometry detection.

2.6. Measurements

Electrochemical analysis of the bioelectrodes was performed using an IM6ex (Zahner Elektrik instruments, Germany) electrochemical work station. A conventional three-electrode system was employed with a saturated calomel electrode (SCE) as the reference electrode, platinum foil as the counter electrode, and the modified GCE (diameter = 3 mm) as the working electrodes. Cyclic voltammetry (CV) measurements were performed in 0.1 M phosphate buffer solution (PBS, pH 7.4) between 0.0 and 1.0 V for characteristic investigations of NF/AChE–CS/Ag NPs–CGR–NF/GCE biosensors. The apparent Michaelis–Menten constant of the biosensor was calculated from the Lineweaver–Burk equation:

$$\frac{1}{i_{ss}} = \left(\frac{K_m^{app}}{i_{max}}\right)\cdot\left(\frac{1}{C}\right) + \left(\frac{1}{i_{max}}\right) \quad (1)$$

where i_{ss} is the steady-state current after the addition of substrate, i_{max} is the maximum current measured under saturated substrate condition and C is the concentration of the substrate. The K_m^{app} is apparent

Michaelis–Menten constant, which gives an indication of the enzyme substrate kinetics for the biosensor, determined by analysis of the slope and intercept of the plot of the reciprocals of steady-state current versus ATCl concentration.

The obtained NF/AChE–CS/Ag NPs–CGR–NF/GCE was first immersed in pH 7.4 PBS containing different concentrations of standard pesticide at room temperature (25 ± 1 °C) for 6 min and then transferred to the electrochemical cell of pH 7.4 PBS containing 0.5 mM ATCl to study the amperometric response by differential pulse (DPV) between 0.2 and 0.75 V. The inhibition of pesticide was calculated as follows:

$$inhibition(\%) = \frac{i_{p,control} - i_{p,exp}}{i_{p,control}} \times 100\% \quad (2)$$

where $i_{p,\,control}$ is the peak current of ATCl on NF/AChE–CS/Ag NPs–CGR/GCE, $i_{p,\,exp}$ is the amperometric response of ATCl on NF/AChE–CS/Ag NPs–CGR/GCE with pesticide inhibition. The detection limit (*LD*) was calculated by using the equation given below [33]:

$$LD = 3S/b \quad (3)$$

where *S* is the standard deviation of the blank solution, *b* is the slope of the analytical curve.

2.7. Precision of measurements and stability studies

The intra-assay precision of the biosensor was evaluated by testing one NF/AChE–CS/Ag NPs–CGR–NF/GCE for six times in 0.5 mM ATCl after being immersed in the 1.0×10^{-10} M chlorpyrifos for 6 min. The inter-assay precision was estimated with six different biosensors in the same way. The intra-assay and inter-assay RSDs demonstrated reproducibility of the biosensor. Stability was evaluated by testing the amperometric response of the NF/AChE–CS/Ag NPs–CGRNF/GCE biosensor in 0.1 M PBS containing 0.5 mM ATCl by CV every five days. The retained ratio of its initial current response indicated the stability of biosensor.

2.8. Preparation and determination of real samples

Two samples, tap water sample and lake water sample, were filtered through a 0.22 μm membrane and the pH was adjusted to 7.4. After simple pretreatment, different concentrations of chlorpyrifos and carbaryl were added to study the recovery under the optimal conditions.

3. Results and discussion

3.1. Characterization of Ag NPs–CGR

Fig. 1 showed the images of CGR and Ag NPs–CGR hybrids. The SEM image of Fig. 1a indicated a few layers of crumpled sheets of CGR morphology with a dimension ranging from several hundred nm to several μm and thickness of 1.1 nm (AFM image Fig. 1S). Fig. 1b image of TEM indicated that Ag NPs were coated on the surfaces of CGR sheets well-separated.

Raman spectra of graphite, GO and CGR were shown in Fig. 2a, respectively. Highly ordered graphite had only a couple of Raman-active bands visible in the spectra, the in-phase vibration of the graphite lattice (G band) at 1576 cm^{-1} as well as the (weak) disorder band caused by the graphite edges (D band) at approximately 1355 cm^{-1}. GO of Raman-active bands visible in the spectra as universal observed that higher disorder in graphite led to a broader G band, as well as to a broad D band of higher relative intensity compared to that of the G band. The G band broadens GO significantly and displayed a shift to higher frequencies of 1357 cm^{-1} and 1601 cm^{-1} (blue-shift), and the D band grew in intensity. CGR of Raman-active bands visible in the spectra shows that the G band shifts back to the position of the G band in graphite, which was attributed to a graphitic "self-healing" similar to what was observed from the sharpening of the G peak and the intensity decrease of the D peak in heat-treated graphite [34]. Raman-active bands were visible in the spectra in accord with reference literature [35].

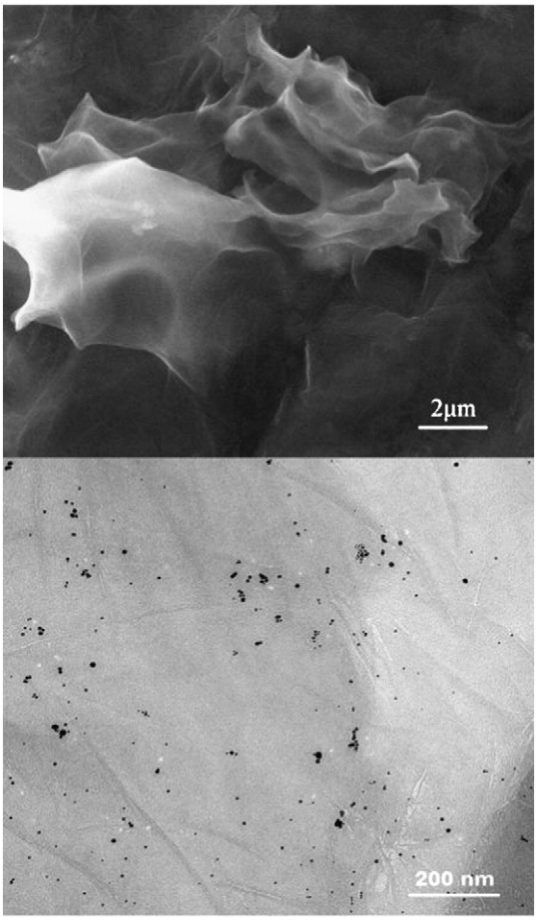

Fig. 1. a. SEM image of CGR. b. TEM image of Ag NPs–CGR.

The formations of GR and CGR were further investigated by FTIR spectra as shown in Fig. 2b. The presence of −OH (3413 cm^{-1}), C═C (1592 cm^{-1}) and C−O (1257 cm^{-1}) ascribed to the stretching vibrations of GR. The appearance of strong peaks at 3404 cm^{-1} and 1733 cm^{-1} on CGR confirmed the presence of the carboxylic group.

Fig. 2c showed the diffraction spectra of CGR and Ag NPs–CGR, respectively. Peaks of the Ag NPs–CGR diffraction spectra could be indicated as Ag NPs which agreed well with the values on the standard card (JCPDS Card No. 04-0783). No other characteristic peaks of the crystalline impurities were observed. Ag NPs–CGR diffraction spectra indicated that Ag NPs were coated on the surfaces of CGR sheets.

3.2. Electrochemical behavior of NF/AChE–CS/Ag NPs–CGR–NF/GCE

CVs were used to investigate the catalysis response of AChE to ATCl on four different biosensors as shown in Fig. 3. No amperometric response could be observed at NF/AChE–CS/GCE (curve a), NF/AChE–CS/GO–NF/GCE (curve b), NF/AChE–CS/CGR–NF/GCE (curve c), and NF/AChE–CS/Ag NPs–CGR–NF/GCE (curve d) in PBS (pH 7.4). However, when 0.5 mM ATCl was added into the PBS (pH 7.4), an obvious amperometric response was observed at NF/AChE–CS/GCE (curve e), NF/AChE–CS/GO–NF/GCE (curve f) NF/AChE–CS/CGR–NF/GCE (curve g) and NF/AChE–CS/Ag NPs–CGR–NF/GCE (curve h). Fig. 3 (curve from e to h) showed that the oxidation peak currents increased and the

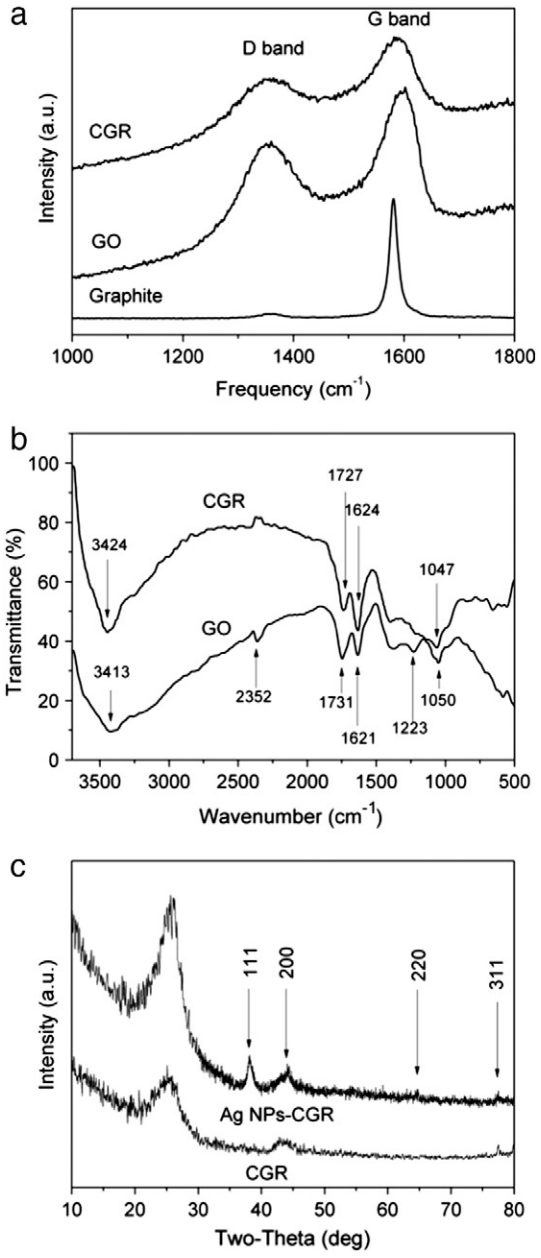

Fig. 2. (a) The Raman spectra of Graphite, GO and CGR; (b) The FTIR spectra of GO and CGR; (c) XRD of CGR and Ag NPs–CGR.

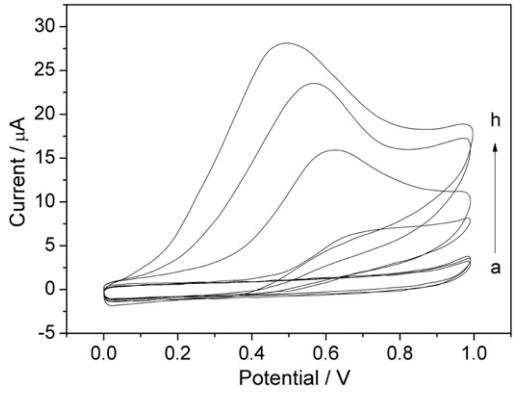

Fig. 3. CV of NF/AChE–CS/GCE (a), NF/AChE–CS/GO–NF/GCE (b), NF/AChE–CS/CGR–NF/GCE (c) and NF/AChE–CS/Ag NPs–CGR–NF/GCE (d) in 0.1 M PBS and in 0.1 M PBS containing 0.5 mM ATCl (e to h), scan rate: 0.10 V/s in 25 °C.

oxidation peak potentials shifted to lower potentials in sequence. The oxidation peak currents increased orderly that indicated the improved conductivity. The oxidation peak potentials shifted to lower potentials orderly that indicated the enhanced catalysis. Obviously, Ag NPs–CGR–NF with excellent conductivity and catalytic activity provided an extremely hydrophilic surface for AChE adhesion. The Ag NPs–CGR–NF possessed excellent conductivity, catalytic activity and biocompatibility which were attributed to the synergistic effects of Ag NPs, CGR and NF. CS was used to immobilize enzymes on the surface of Ag NPs–CSNS–NF/GCE, keep the enzyme activities and improve electrons to shuttle between the enzyme and the electrode. Besides, NF protective membrane was used to prevent the loss of the enzyme molecules, improve the anti-interference ability of the biosensor and provide a biocompatible microenvironment to maintain enzymatic activity.

3.3. Detection of ATCl

Under optimal conditions (see Supplementary), CVs were used to investigate the electrochemistry reaction between AChE and ATCl. Fig. S5 showed the calibration curves for ATCl determination. With increasing ATCl concentration, the amperometric response of the biosensor increases. The amperometric response of the biosensor was a linear function of ATCl concentration in two segments. One was from 1 μM to 50 μM and the other was from 50 μM to 500 μM. The detection limit was 0.5 μM. At higher ATCl concentrations the shape of the amperometric response was indicative of a Michaelis–Menten process (Fig. S5). The K_m^{app} in the present studies was calculated to be 133 μM according to the Lineweaver–Burk equation. This value was lower than that for AChE adsorbed on reduced graphene oxide–gold nanocomposite modified electrode (0.16 mM) [36], for AChE immobilized on CdS-decorated graphene nanocomposite modified electrode (0.24 mM) [37] and for AChE adsorbed on liposome bioreactors–chitosan nanocomposite film modified electrode (0.36 mM) [38] indicating that the NF/AChE–CS/Ag NPs–CGR–NF/GCE biosensor had a great affinity and catalysis to its substrate ATCl.

3.4. Effect of incubation time

Inhibition of chlorpyrifos and carbaryl were tested by CV in terms of their effect on AChE activity at different incubation times (2 to 16 min) in a pesticide solution (10^{-10} M), respectively. The inhibition level of AChE increased with increasing incubation time (Fig. S7). Considering the relations of analytical time with sensitivity and stability of the amperometric measurements, an exposure time of min was chosen as the best compromise between the signal and exposure time.

3.5. Pesticide detection

The inhibition effects of different pesticides were investigated by DPV measuring the response of the biosensor to 0.5 mM ATCl after incubation by different concentrations of chlorpyrifos and carbaryl, respectively. As shown in Fig. 4, with the response of the biosensor before and after 6 min of incubation in 10^{-13}, 10^{-12}, 10^{-11}, 10^{-10}, 10^{-9} and 10^{-8} M chlorpyrifos, the peak currents (curves b–g) dramatically decreased compared with that on the control (curve a), and the decrease in peak current increased with the increasing concentration of chlorpyrifos. Calibration plots of inhibition percentage versus pesticide concentration were shown in Fig. 5. Linear relationships between the inhibition percentage and the concentration of pesticides were obtained as shown in Table S1. The two linear ranges of chlorpyrifos and carbaryl indicated that the biosensor was more sensitive for detecting low concentration of pesticides than high concentration of pesticides.

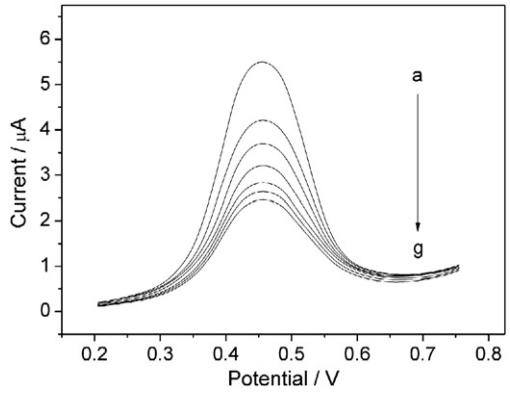

Fig. 4. DPV of the NF/AChE–CS/Ag NPs–CGR–NF/GCE in 0.1 M PBS containing 0.5 mM ATCl after incubation with 0 (a), 10^{-13} M (b), 10^{-12} M (c), 10^{-11} M (d), 10^{-10} M (e), 10^{-9} M (f) and 10^{-8} M (g) chlorpyrifos for 6 min.

3.6. Interference study

The interfering signal due to the most common electroactive species was investigated. The signal for a fixed concentration of ATCl was compared with the signal obtained in the presence of the interfering species after the biosensor was incubated in 10^{-10} M chlorpyrifos for 6 min. The test result shows that no noticeable changes of amperometric response were detected in the presence of 0.5 mM glucose, 0.5 mM citric acid and 0.5 mM oxalic acid respectively at the present operating potential in this system. However, the amperometric response decreased obviously in the presence of 0.5 mM p-nitrophenol, 0.5 mM nitrobenzene, 0.5 mM p-nitroaniline, 0.5 mM trinitrotoluene, 0.5 mM toluene, 0.5 mM p-toluenesulfonic acid and 10^{-10} M carbaryl. The results of the interference study were shown in Fig. S7.

3.7. Precision of measurements and stability of biosensor

The intra-assay precision of the biosensors was evaluated by assaying one enzyme electrode for six replicate determinations in 0.5 mM ATCl after being immersed in 1.0×10^{-10} M chlorpyrifos for 6 min. Similarly, the inter-assay precision, or fabrication reproducibility, was estimated at six different electrodes. The RSDs of intra-assay and inter-assay were found to be 3.7% and 5.9%, respectively, indicating an acceptable reproducibility. When the enzyme electrode was not in use, it was stored at 4 °C condition. No obvious decrease in the response of ATCl was observed in the first 10-day storage. After a 30-day storage period, the sensor retained 88% of its initial current response, indicating the acceptable stability of biosensor.

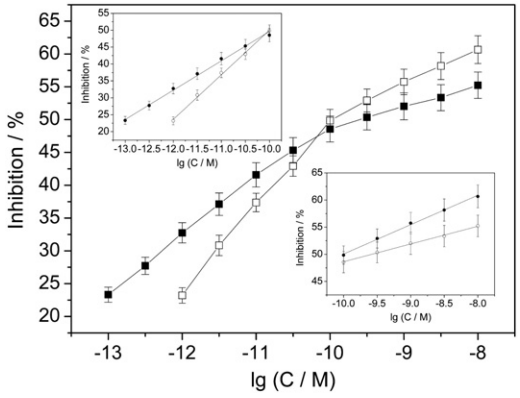

Fig. 5. Inhibition curves of NF/AChE–CS/Ag NPs–CGR–NF/GCE biosensor for chlorpyrifos and carbaryl determination by DPV.

3.8. Analytical real samples

To investigate the accuracy of an analytical method, spike recovery is a useful tool. The variability was low if there were no interferences or matrix effects so that recovery close to 100% was expected. A standard addition method was adopted to estimate the accuracy. Table S2 showed the results obtained by analysis of these spiked samples. The recoveries of tap water and lake water were observed in the range of 93.1–105.6%, which demonstrated low matrix effect on the amperometric response. The low relative standard deviations for chlorpyrifos and carbaryl demonstrated the high precision of analysis.

4. Conclusion

In this work, combining the advantageous characteristics of Ag NPs and CGR, NF and CS, a novel AChE biosensor based on Ag NPs–CGR–NF has been developed. The biosensor exhibited many advantages, such as low applied potential, fast response, high sensitivity, acceptable stability, reproducibility and simple fabrication. The biosensor has potential application in biomonitoring of chlorpyrifos and carbaryl pesticides and other organophosphate and carbamate pesticides. The method not only can be used to immobilize other enzymes to construct a range of biosensors but also may be extended to assemble other biological molecules, such as antibody, antigen and DNA for wide bioassay applications.

Acknowledgment

This work was supported by the Natural Science Foundation of China (31160334) and the Natural Science Foundation of Yunnan Province (2012FB112), People's Republic of China.

Appendix A. Supplementary data

Supplementary data to this article can be found online at http://dx.doi.org/10.1016/j.msec.2013.10.036.

References

[1] F. Saez, C. Pozo, M.A. Gomez, M.V. Martinez-Toledo, B. Rodelas, J. Gonzalez-Lopez, Appl. Microbiol. Biotechnol. 71 (2006) 563–567.
[2] R.A. Videira, M.C. Madeira, V.I. Lopes, V.M. Madeira, Biochim. Biophys. Acta 1511 (2001) 360–368.
[3] N.A. Hosea, H.A. Berman, P. Taylor, Biochemistry 34 (1995) 11528–11536.
[4] S. Andreescu, J.L. Marty, Biomol. Eng. 23 (2006) 1–15.
[5] K.S. Novoselov, A.K. Geim, S.V. Morozov, D. Jiang, Y. Zhang, S.V. Dubonos, I.V. Grigorieva, A.A. Firsov, Science 306 (2004) 666–669.
[6] M.D. Stoller, S.J. Park, Y.W. Zhu, J.H. An, R.S. Ruoff, Nano Lett. 8 (2008) 3498–3502.
[7] A.K. Mishra, S. Ramaprabhu, J. Phys. Chem. C 115 (2011) 14006–14013.
[8] E. Yoo, J. Kim, E. Hosono, H.S. Zhou, T. Kudo, I. Honma, Nano Lett. 8 (2008) 2277–2282.
[9] J. Xiao, D. Mei, X. Li, W. Xu, D. Wang, G.L. Graff, W.D. Bennett, Z. Nie, L.V. Saraf, I.A. Aksay, J. Liu, J.G. Zhang, Nano Lett. 11 (2011) 5071–5078.
[10] B. Seger, P.V. Kamat, J. Phys. Chem. C 113 (2009) 7990–7995.
[11] R. Kou, Y.Y. Shao, D.H. Wang, M.H. Engelhard, J.H. Kwak, J. Wang, V.V. Viswanathan, C.M. Wang, Y.H. Lin, Y. Wang, I.A. Aksay, J. Liu, Electrochem. Commun. 11 (2009) 954–957.
[12] X. Wang, L.J. Zhi, N. Tsao, Z. Tomovic, J.L. Li, K. Mullen, Angew. Chem. Int. Ed. 47 (2008) 2990–2992.
[13] J.B. Wu, H.A. Becerril, Z.N. Bao, Z.F. Liu, Y.S. Chen, P. Peumans, Appl. Phys. Lett. 92 (2008) 263302–263303.
[14] S.J. Guo, S.J. Dong, J. Mater. Chem. 21 (2011) 18503–18516(18).
[15] X.Y. Yang, X.Y. Zhang, Y.F. Ma, Y. Huang, Y.S. Wang, Y.S. Chen, J. Mater. Chem. 19 (2009) 2710–2714.
[16] Y. Wang, S. Zhang, D. Du, Y.Y. Shao, Z.H. Li, J. Wang, M.H. Engelhard, J.H. Li, Y.H. Lin, J. Mater. Chem. 21 (2011) 5319–5325.
[17] J.D. Qiu, J. Huang, R.P. Liang, Sens. Actuators B 160 (2011) 287–294.
[18] S.S. Han, H. Kim, N. Park, J. Phys. Chem. C 115 (2011) 24696–24701.
[19] R.F. Nie, J.H. Wang, L.N. Wang, Y. Qin, P. Chen, Z.Y. Hou, Carbon 50 (2012) 586–596.
[20] S. Stankovich, D.A. Dikin, G.H.B. Dommett, K.M. Kohlhaas, E.J. Zimney, E.A. Stach, R.D. Piner, S.T. Nguyen, R.S. Ruoff, Nature 442 (2006) 282–286.
[21] D. Li, R.B. Kaner, Science 320 (2008) 1170–1171.
[22] M.X. Kan, X.J. Wang, H.M. Zhang, Chin. Chem. Lett. 22 (2011) 458–460.
[23] X. Ren, X. Meng, D. Chen, F. Tang, J. Jiao, Biosens. Bioelectron. 21 (2005) 433–437.
[24] C. Ren, Y. Song, Z. Li, G. Zhu, Anal. Bioanal. Chem. 381 (2005) 1179–1185.

[25] Z.P. Chen, Z.F. Peng, Y. Luo, B. Qu, J.H. Jiang, X.B. Zhang, G.L. Shen, R.Q. Yu, Biosens. Bioelectron. 23 (2007) 485–491.
[26] F.Y. Hsu, D.S. Yu, J.C. Chang, C.L. Chuang, J. Chin. Chem. Soc. 58 (2011) 756–760.
[27] A. Sassolas, L.J. Blum, B.D. Leca-Bouvier, Biotechnol. Adv. 30 (2012) 489–511.
[28] X.H. Kang, Z.B. Mai, X.Y. Zou, P.X. Cai, J.Y. Mo, Anal. Biochem. 369 (2007) 71–79.
[29] C.A. Lee, Y.C. Tsai, Sens. Actuator B 138 (2009) 518–523.
[30] N.E. Azmi, M. Ahmad, J. Abdullah, H. Sidek, L.Y. Heng, N. Karuppiah, Anal. Biochem. 388 (2009) 28–32.
[31] W.S. Hummers, R.E. Offeman, J. Am. Chem. Soc. 80 (1958) 1339-1339.
[32] X.M. Sun, Z. Liu, K. Welsher, J.T. Robinson, A. Goodwin, S. Zaric, H.J. Dai, Nano Res. 1 (2008) 203–212.
[33] Analytical Methods Committee, Analyst 112 (1987) 199–204.
[34] K. Sato, R. Saito, Y. Oyama, Chem. Phys. Lett. 427 (2006) 117–121.
[35] K.N. Kudin, B. Ozbas, H.C. Schniepp, R.K. Prud'homme, I.A. Aksay, Nano Lett. 8 (2008) 36–41.
[36] T. Liu, H.C. Su, X.J. Qu, P. Ju, L. Cui, S.S. Ai, Sens. Actuator B 160 (2011) 1255–1261.
[37] K. Wang, Q. Liu, L.n. Dai, J.J. Yan, C. Ju, B.J. Qiu, X.Y. Wu, Anal. Chim. Acta. 695 (2011) 84–88.
[38] H.N. Guan, F.L. Zhang, J. Yu, D.F. Chi, Food Res. Int. 49 (2012) 15–21.